ORIGINAL ARTICLE

Neutralization of SARS-CoV-2 Spike Pseudotyped Viruses Using Postbiotic Preparations from *Lactiplantibacillus plantarum* BS25

Joshua Angelo Hermida Mandanas,[1,2] Day Yu-Chao[2,3] and Leslie Michelle M. Dalmacio[1]

[1]*Department of Biochemistry and Molecular Biology, College of Medicine, University of the Philippines Manila, Manila, Philippines*
[2]*Graduate Institute of Microbiology and Public Health, National Chung Hsing University, Taichung, Taiwan*
[3]*Institut Pasteur, Paris, France*

ABSTRACT

Background. Despite the presence of SARS-CoV-2 antivirals, namely, remdesivir, nirmatrelvir and toremifene, these drugs entail adverse effects and limited effectiveness. Thus, development of a safer alternative is imperative, and likely candidates include the cell-free supernatant (CFS) and protein fractions from *Lactiplantibacillus plantarum* strains. These postbiotics have known antiviral properties primarily mediated by plantaricins and enhanced by organic acids.

Objectives. The study determined the *in silico* mechanism of plantaricins against the receptor-binding domain (RBD) and angiotensin-converting enzyme 2 (ACE2), as well as compared the *in vitro* activities of the *L. plantarum* BS25 CFS, semi-purified and crude protein fractions, against the SARS-CoV-2 pseudotyped viruses (nCoV-S-EGFP) expressing the spike of wild-type (wt) Wuhan strain, Omicron BA.1 and BA.4/5 variants. Further, this study determined the metabolome of the strain BS25 CFS.

Methods. A quasi-experimental approach was utilized in the study. Plantaricins were screened for safety *in silico*, followed by molecular docking with RBD and ACE2. Using a cell culture model, two-fold dilutions of the CFS and fractions were tested for cytotoxicity and microneutralization against the pseudoviruses. Mass spectrometry was utilized for the metabolomics.

Results. Plantaricins interact stably with RBD than ACE2 which were mediated by hydrogen, hydrophobic and covalent bonds. The activities of the CFS and fractions were substantially higher against the nCoV-S-EGFP BA.4/5 variant. The 1:8 dilution of CFS entailed no cytotoxicity and displayed higher activities than toremifene. Metabolomics has identified a relatively abundant putative peptide, followed by organic acids and cyclic peptides.

Conclusion. Plantaricins can prevent SARS-CoV-2 entry by interacting with key RBD mutations or with intrinsically disordered RBD residues. The cationic and hydrophobic RBD mutations in the BA.4/5 variant may facilitate interactions with the putative peptide from the CFS and fractions, hence the observed potent activities. These findings can be used as basis for the development of an alternative antiviral targeting the RBD of live or pseudotyped SARS-CoV-2 variants.

Keywords: Lactiplantibacillus plantarum, *SARS-CoV-2*, *cell-free supernatant*

eISSN 2094-9278 (Online)
Published: April 16, 2026
https://doi.org/10.47895/amp.vi0.13453

Corresponding author: Joshua Angelo Hermida Mandanas
Department of Biochemistry and Molecular Biology
College of Medicine
University of the Philippines Manila
547 Pedro Gil St., Ermita, Manila 1000, Philippines
Email: jhmandanas@up.edu.ph
ORCiD: https://orcid.org/0000-0002-4590-9483

INTRODUCTION

SARS-CoV-2 caused the previous pandemic, coronavirus disease 2019 (COVID-19), which still poses public health risks.[1] Among its components, the spike RBD mediates entry to susceptible host cells and is an important target for development of therapeutics.[2-4] Majority of mutations in the previous SARS-CoV-2 variants of concerns, *i.e.,* Omicron BA.1 and BA.4/5, were found in the RBD and linked with disease severity.[5]

Currently, the Food and Drug Administration (FDA) has approved antiviral drugs mostly targeting the SARS-CoV-2 enzymes which reduces risks of hospitalization or death. These include remdesivir and molnupiravir, which targets the RNA polymerase, while nirmatrelvir targets the protease. An FDA-repurposed drug, toremifene, has been evaluated *in vitro* to inhibit SARS-CoV-2 entry.[6] These drugs entail adverse effects, high cost, limited effectiveness, and availability. Remdesivir is not recommended beyond 7-10 days, molnupiravir is ineffective to Omicron variants while nirmatrelvir increase symptom recurrences.[7-9] The adverse effects of toremifene can be noticed within 3-5 days of intake and a clinical trial has been withdrawn in 2021.[10] In the Philippines, monoclonal antibodies have been suggested as alternative antivirals, which include casirivimab (REGN 10933) and imdevimab (REGN 10987), however these were ineffective against Omicron variants.[11] With these drawbacks, a safer alternative antiviral capable of targeting the RBD can be developed.

Promising candidates would be postbiotics, which were the functional bioactive compounds from preparations including the cell-free supernatant (CFS) of probiotics such as *Lactiplantibacillus plantarum*, known to contain antiviral metabolites.[12] They also include metabolites, lysates, secretions and other components which endow fitness directly or indirectly to both probiotics and humans, and their use offer advantages compared to probiotics, as they entail ease of optimization, stability and does not involve colonization.[12] Among the CFS metabolites, plantaricins (Pln), which were bacteriocins composed of cationic or hydrophobic residues known to bind with target receptors or permeabilize lipid membranes, mostly mediate the activity.[13,14] The CFS from the strain *L. plantarum* BS25 has been known to produce a potent bacteriocin. These were ribosomally synthesized antimicrobial peptides of bacteria and archea.[15] Recent data from its whole genome sequence indicates that it can produce plantaricins similar to Pln K, E, F, S and Y.[16] Pln E and F have been identified *in silico* to interact with SARS-CoV-2 helicase.[14] The lanthipeptide Pln W has also been determined *in silico* to interact with both RBD and ACE2.[17] Organic acids found in the CFS can enhance the activity by causing conformational changes to viral proteins or increase membrane permeability.[18] Most of the *in vitro* activities of CFS from *L. plantarum* strains were observed upon coincubation with RNA viruses, such as SARS-CoV-2, HIV, echovirus, coxsackievirus, transmissible gastroenteritis virus and influenza.[13,14,19-22] *In silico* interactions of plantaricins against SARS-CoV-2, HIV and influenza were also noted.[13,14,22] However, to this end, there were no studies exploring the activity of CFS and its semi-purified or crude protein fractions against SARS-CoV-2 pseudoviruses expressing the spike of the basal strain and variants of concern. Emphasis is also highlighted on the search for putative peptides as antivirals, albeit a possible cytotoxicity is inevitable.

MATERIALS AND METHODS

In silico Safety Evaluation of Plantaricins

Plantaricins (Pln) composed of 5-35 residues and have known antimicrobial activities were obtained from PDB, Pubchem and databases (https://aps.unmc.edu/database/result; http://dramp.cpu-bioinfor.org) from September 2021-January 2023. The search keywords used were "plantaricin," "plantaricins," "bacteriocins," "producing strain-*Lactobacillus plantarum* or *Lactiplantibacillus plantarum,*" "additional properties– antimicrobial, antiviral, antibacterial." The safety evaluation was performed in ADMET 2.0 (https://admet.scbdd.com/calcpre/index/#).[23] Plantaricins which passed the safety profiling proceeded with docking analysis.

In silico Docking of Plantaricins with RBD and ACE2

This was done to describe the antiviral mechanism of plantaricins from *L. plantarum* strains in terms of blocking the RBD and ACE2 to prevent entry in cells. Also, this can support the potential mechanism of the putative peptide, possibly a plantaricin, from the strain BS25. RBD-binding residues of ACE2 (PDB 2AJF), as well as the RBD of the Wuhan strain (PDB 6VYB), Delta (PDB 7V7Q), UK (PDB 7LWV), South African (PDB 7LYN), D614G (PDB 7KDL) and Omicron variants, BA.1.1.529 (PDB 7TL9), BA.1 (PDB 7T9L) and BA.4/5 (PDB 7XNQ), were utilized. Plantaricins without available structures were processed in I-Tasser (https://zhanggroup.org/I-TASSER/). Each structure of plantaricin, ACE2 and RBD underwent removal of ligands, ions or water using UCSF Chimera 1.16, and energy minimization through Yasara (http://www.yasara.org/). Each model quality was checked in the Ramachandran plot (https://zlab.umassmed.edu/bu/rama/). GlobPlot 2 (http://globplot.embl.de/) was utilized for predictions of intrinsically disordered regions (IDR). Docking was performed in ClusPro 2.0 (https://cluspro.bu.edu/) and structures were obtained from clusters with the lowest "balanced" energy, which represent the most likely model of the interactions.[24] Atomic and molecular interactions were evaluated using Chimera. The binding affinity and dissociation constant (K_d) of the best candidate plantaricin was processed in PRODIGY (https://wenmr.science.uu.nl/prodigy/), with the temperature reflecting the respiratory epithelium (35°C).[25]

Preparation of the Strain BS25 Cell-Free Supernatant (CFS)

Institutional permits (*e.g.,* Research Grants Administration Office, Institutional Biosafety and Biosecurity Committee, Research Ethics Board) were initially prepared prior to working in the laboratory. The probiotic culture, induction of specific conditions to prepare the CFS, semi-purified fractions and metabolomics samples were done in the BSL-1 Graduate Laboratory of the Department of Biochemistry and Molecular Biology (DBMB), University of the Philippines Manila (UPM). The strain BS25, sourced from a locally-fermented food, Balao balao, has a glycerol stock provided by the UP Manila Applied Microbiology for Health and Environment Research Group (AMHERG). Microaerophilic conditions were utilized during bacterial culture.[26] 6 x 10^6 CFU/mL was inoculated into a 50 mL MRS broth and incubated for 14 hrs at 37°C.[27] Then, 25 mL was inoculated in 1 liter MRS broth for further incubation at 32 hrs. Optimized conditions for the isolation of plantaricins were followed.[15,28,29] Each supernatant was heated at 70°C for 30 mins and syringe-filtered (0.22 µm, PES) to remove contaminating proteins and isolate plantaricins of class I or class II bacteriocins.[14,17,28,29] The pH of the CFS was maintained at pH 4.0.

Preparation of the Semi-purified and Crude Protein Fractions from the CFS

A 100 mL CFS aliquot was saturated with 70% of 0.01 M ammonium sulphate at 4°C and pooled to obtain the precipitate (labeled as ASP, **A**mmonium **S**ulphate **P**recipitate of the CFS) diluted in 100 mL of 0.01 M PBS (pH 6.0). 2 mL from this was sterile-filtered and loaded in Sephadex G25 column (16.17 mm x 90 mm, Sigma-Aldrich, Cytiva™) equilibrated with distilled water followed by washing with 0.01 M PBS (pH 6.0, 25°C). The flow rate was 2 mL/min. There were 35 gel-purified fractions with only Fractions #5, #6, #9, #31, #33, #35 obtaining the highest activity against the preliminary indicator strain, *Streptococcus mutans*. These were pooled (52.2 mg) in the Central Instrumentation Facility – De La Salle University (CIF-DLSU) for the semi-preparative RP-HPLC. Among these fractions, only Fraction (#8) (labeled as HAP8, RP-**H**PLC Fraction no. **8** from the **A**mmonium Sulphate **P**recipitate) was utilized as it has a detectable protein and *de novo* sequence. Also, only the gel chromatography-purified Fractions #5, #6 and #9 were pooled into one sample (labeled as GAP, **G**el chromatography fractions from the **A**mmonium Sulphate **P**recipitate) as it has activity against *S. mutans*, detectable protein and SDS-PAGE bands. To this end, the semi-purified fractions prepared successively from the CFS which were tested for the *in* vitro assays include the ASP, followed by GAP then by HAP8. The single protein bands (crude protein fraction) from the tris-tricine SDS-PAGE (**S**DS **G**el-**E**xcised) of CFS (SGE-CFS) and ASP (SGE-ASP) were excised and also tested for the *in vitro* assays to support if the activity is primarily mediated by a peptide.[30]

Screening for the Presence of Plantaricins

This includes a detectable protein content, non-lethality to the producing probiotic strain and broad antimicrobial activity.[15,31] *S. mutans* was utilized as a preliminary indicator strain due to previous accessibility and is also known to be susceptible to the activity of plantaricins.[32] Absence of the zone of inhibition (ZOI) against the BS25 indicates the presence of plantaricins, as producing strains entail blocking proteins or channels.[31] Confirmation using an actual plantaricin control peptide was not performed.

Protein Concentration and Tris-tricine SDS PAGE

The *in vitro* assays which include tris-tricine SDS-PAGE (sodium dodecyl sulfate-polyacrylamide gel electrophoresis), MTT (3-(4,5-Dimethylthiazol-2-yl)-2,5-diphenyl tetrazolium bromide) and nCoV-S-EGFP micro-neutralization assays, respectively, were all performed in the BSL-2 Virology Laboratory of the Graduate Institute of Microbiology and Public Health (GIMPH), National Chung Hsing University (NCHU), Taichung, Taiwan. A Material Transfer Agreement was secured to transport the CFS and semi-purified fractions, MRS agar and broth, as well as the control drug for the microneutralization assay, toremifene citrate, towards the NCHU. The Qubit assay and SDS-PAGE was performed using the manufacturer's manual (Thermo Fisher and BioRad). Vertical electrophoresis gels were set at 100-120 volts. A non-reducing setup was utilized which included a "spacer" gel placed between the stacking and resolving gels to increase the resolution of peptides between 1-5 kDa.[33] 25 µL of 2 mg bovine serum albumin was the control along with 7µL ladder (Thermo Scientific, 10-180 kDa).

Strain BS25 CFS Metabolome

This was performed to profile BS25 CFS metabolites with known functional properties and to check the consistency of the CFS preparation based on the literatures, in which plantaricins and organic acids predominate.[14,18] All mass spectrometry samples were processed in the Central Instrumentation Facility (CIF) of De La Salle University (DLSU), Laguna. A 15 mL CFS aliquot underwent mass spectrometry using the protocol from Wang et al.[34] An optimization step (Agilent InfinityLab LC series Infinity II Semi-prep HPLC with VWD detector, Quaternary HPLC system) using a linear gradient of 0.1% formic acid in ultrapure water and 0.1% formic acid in methanol was utilized, followed by the Ultra-high Performance Liquid Chromatography-Tandem Mass Spectrometry with Quadrupole Time of Flight Reaction (UHPLC-MS/MS-qTOF, Agilent 1260 Infinity II HPLC with 6530 QTOF LCMS detector, Poroshell 120 EC-C18 3.0 x 150 mm 2.7 micron) performed at 23°C with an injection volume of

450 µL and flow rate of 30 mL/min by a linear gradient of 0.1% formic acid in ultrapure water and 0.1% formic acid in MS grade acetonitrile. Mass range for MS is 10-2000 Daltons (Da) while MS/MS is between 50-2000 Da. Data were submitted in Global Natural Products Social Molecular Networking (GNPS) database and hits were confirmed in Microbial Metabolite Database (MiMeDB)(https://mimedb.org/), Pubchem, or ChemSpider. Metabolites with potential impacts on cell viability and antiviral activity were quantified through their ion abundances by an in-house data-dependent acquisition (DDA) method (CIF-DLSU).

Mass Spectrometry of the Suspect Compound

The pooled gel-purified fractions underwent semi-preparative HPLC (Agilent 1260 InfinityLab LC series 1260 Infinity HPLC with VWD detector, C18 30 x 150 mm and 10 µm pore). The mobile phase used is a linear gradient of 0.1% formic acid in MS grade methanol and 0.1% formic acid in ultrapure water. The injection volume is 450 µL with a flow rate of 30 mL/min. MS range is 100-2000 Da while for MS/MS, 50-2000 Da. Spectral reading was performed to both 254 nm and 280 nm. This was followed by UHPLC-ESI-MS/MS-qTOF performed at 23˚C with an injection volume of 5 µL and flow rate of 0.4 mL/min. A linear gradient of 0.1% formic acid in ultrapure water and 0.1% formic acid in acetonitrile was utilized. Mass range for both MS and MS/MS was searched between 100-2000 Da. Data were initially submitted in the Mascot web server (https://www.matrixscience.com/), GNPS, and DenovoGUI softwwere. *De novo* sequencing was performed using PEAKS DB.[35,36] The binding affinity of the suspect or putative peptide against the ACE2 and RBD of the Wuhan strain, BA.1 and BA.4/5 variants, was also processed in PRODIGY. Toremifene, as a control, was processed in Autodock Vina since it is a non-peptide ligand.

Cytotoxicity Assay

HEK293T-hACE2, an epithelial cell line derived from a human embryonic kidney, overexpressing the ACE2 and contains a plasmid for blasticidin resistance, was utilized for both MTT and microneutralization assays. The samples tested in these assays included the CFS and its semi-purified fractions, namely, ASP, GAP and HAP8, respectively, as well as the crude protein fractions, SGE-CFS and SGE-ASP.

The MTT assay was done to determine which two-fold dilutions, namely 1:2, 1:4 and 1:8, promoted viability and cytotoxicity to the cell line (which reflects the cell type infected by SARS-CoV-2). Two-fold dilutions starting from 60 µL of DMEM-F12-10%FBS, added with an equal amount of sample and 30 µL were serially diluted. Background correction was performed by subtracting the average absorbance value of the blank from each sample and controls. The positive control in all runs included the wells containing cells with complete media only while the blank includes the wells containing only the complete media, whereas the negative control were the wells containing cells treated with phosphate buffer saline.[37]

Microneutralization Assay

This assay was done to determine the blocking or neutralization of a pseudovirus entry into a cell line by the two-fold dilutions, namely 1:2, 1:4 and 1:8. Each pseudovirus, namely the nCoV-S-EGFP wt Wuhan, Omicron BA.1 and BA.4/5 variants, were acquired from the RNAi Core Facility of Academia Sinica and expresses the enhanced green fluorescent protein (EGFP) from which a fluorescence intensity (FI) can be detected upon a single-round infection to the cell line. The protocol similar to Rather et al. was utilized.[14] Proteolytic treatment using Dithiothreitol and Trypsin-lysC were added to both CFS and ASP which were tested against the nCoV-S-EGFP BA.4/5 variant.[28] The antiviral activity pertains to the percent inhibition of EGFP FI upon treatment with the samples. A dilution is considered neutralizing if it causes an inhibition by 50% or higher. Toremifene citrate was used as the control. EGFP FI was detected using 485 nm excitation and 520 nm wavelength (FLUOstar OPTIMA, BMG). The positive control is toremifene citrate-treated cells, while the negative control is cells treated with complete media. Background correction was done by subtracting the average absorbance value (RFU/µL) of the blank (complete media) from the samples. The following equation was used to determine the percent inhibition.[38]

Formula no. (1):

$$\frac{(\text{RFU}/\mu\text{L}^{1} \text{ of virus control}^{2}) - (\text{RFU}/\mu\text{L sample})}{(\text{RFU}/\mu\text{L of virus control})}$$

[1] relative fluorescence units per µL of EGFP fluorescence intensity, and; [2] virus control (cells in complete media and pseudovirus).

Statistical Analysis

Statistical analysis and data representations were performed through GraphPad Prism (v10.0). Demographic statistics was utilized for the summative and graphical visualizations. For the inferential analysis, the unpaired t-test was performed for the comparison of antiviral activity, cell viability or toxicities. The relationship of two significant variables was analyzed through Pearson correlation. For the MTT assay, a curve-fitting nonlinear regression was used to identify the CC50, defined as the concentration producing a response halfway between the range of a baseline and maximum value, *i.e.,* the median concentration in which only half of the population of cells were viable. Also, this nonlinear regression was performed in the microneutralization to determine the IC50, or the minimum inhibitory concentration where the EGFP FI decreased by 50%. Across the analysis for these assays, the level of significance was set at 0.05, and is significant if $p < 0.05$. Statistical significance using

the GraphPad style were indicated in figures, these include ns (not significant), * (p <0.05), ** (p <0.01), *** (p <0.001), and **** (p <0.0001). Error bars depicted in the following figures indicate the mean ± SEM (standard error of mean).

Table 1. *In silico* Safety Evaluation of Selected 17 plantaricins

Bacteriocin class	Plantaricin (Pln) (n=17)	Passed ADMET[1] (17/17)	Predicted as intranasal drug (6/17)
I (lanthipeptide)[2]	α-Pln W	✓	✓
	β-Pln W	✓	✗
	C	✓	✗
I	149	✓	✓
II	NC8	✓	✓
	3	✓	✗
	GZ1-27	✓	✗
	A	✓	✗
	α-Pln S	✓	✗
	β-Pln S	✓	✗
	J	✓	✗
	DL3	✓	✓
	E	✓	✗
	F	✓	✓
	ZJ5	✓	✓
	KL-1Y	✓	✗
	Y	✓	✗

[1] *ADMET (Absorption, Distribution, Metabolism, Excretion, Toxicity)*

[2] *Peptides with post-translational modification composed of thioether links between dehydrated serines and threonines with dehydrated cysteines*

RESULTS

In silico Safety Evaluation

There were 17 plantaricins selected across several databases and Table 1 shows their safety profile. All were predicted to entail low toxicities and have no mutagenic potential. Among these, only Pln DL3, F, NC8, 149, ZJ5 and the α-subunit of Pln W, have been predicted as potential intranasal drugs. To identify their antiviral mechanism, interactions with the RBD and ACE2 have been explored through molecular docking.

In silico Docking of Plantaricins with RBD and ACE2

All 3D models have residues in the highly preferred observations, hence suitable for docking (Table 2). The mean binding energy (kCal/mol) with RBD (mean ± SEM, n=number of interacting Pln), were as follows, Wuhan strain (-897.45 ± 26.77, n=10), South African variant (-983.87 ± 32.24, n=14), UK variant (-846.23 ± 184.78, n=11), D614G variant (-716.85 ± 30.97, n=13), Delta variant (-987.14 ± 41.85, n=12), Omicron BA.1.1.529 (-904.79 ± 41.56, n=13), BA.1 (-925.37 ± 39.04, n=12) and BA.4/5 variants (-1004.33 ± 68.99, n=8). The mean binding energy with ACE2 is -897.3 ± 57.01 (n=8). The α-Pln W obtained the lowest binding energy especially for the Omicron BA.4/5 variant RBD (-1308.3).

Among the 17 Pln, there were only 6 capable of interacting with the key RBD mutations (Table 3). Interaction

Table 2. *In silico* Interactions of each plantaricin with ACE2 and RBD

Plantaricin (Pln) (n=17)	ACE2 receptor (8/17)	Wuhan strain (10 /17)	South African (14/17)	SARS-CoV-2 RBD basal strain or variants				Omicron BA. 1.1.529 (13/17)	Omicron BA.4/5 (8/17)
				UK (11/17)	D614G (13/17)	Delta (12/17)	Omicron BA.1 (12/17)		
α-Pln W	✓	✓	✓	✓	✓	✓	✓	✓	✓
β-Pln W	✓	✓	✓	✓	✓	✓	✓	✓	✓
C	✓	✓	✓	✗	✓	✓	✓	✓	✓
149	✗	✓	✓	✗	✓	✗	✗	✓	✗
NC8	✗	✓	✓	✓	✓	✗	✓	✗	✗
3	✓	✓	✓	✓	✓	✓	✓	✓	✓
GZ1-27	✓	✗	✗	✗	✓	✓	✓	✓	✓
A	✗	✗	✗	✓	✗	✗	✓	✓	✗
β-Pln S	✓	✗	✓	✗	✗	✓	✗	✗	✗
α-Pln S	✗	✗	✓	✓	✓	✓	✓	✓	✓
J	✓	✓	✓	✓	✓	✓	✓	✗	✗
DL3	✗	✗	✗	✓	✓	✗	✗	✗	✓
E	✗	✗	✓	✓	✗	✓	✗	✓	✗
F	✓	✓	✓	✓	✓	✓	✓	✓	✓
ZJ5	✗	✓	✓	✗	✗	✗	✗	✓	✗
KL-1Y	✗	✓	✓	✗	✓	✓	✓	✓	✗
Y	✗	✗	✓	✓	✓	✓	✓	✓	✗

with these mutations blocks access to ACE2 which can lead to prevention of viral entry.[39] The mean atomic distance (Å) from these interactions is 2.021 ± 0.1 (mean ± SEM) (n=8). Majority of the interactions were from class I and lanthipeptides mediated by their hydrophobic residues. Also, there were only 7 Pln which mediated covalent interactions with the RBD (Table 4). The mean atomic distance (Å) from these covalent bonds is 3.00 ± 0.17 (mean ± SEM) (n=10).

Covalent bonds are formed when electrons are shared in the orbitals making these stronger than hydrogen or hydrophobic interactions.[40] Further, there were only 8 Pln capable of interacting with ACE2 (Table 5). This interaction blocks the access of RBD which also leads to prevention of entry. The mean atomic distance (Å) of interactions with ACE2 is 2.22 ± 0.89 (mean ± SEM) (n=22). Majority of the interacting residues were polar or solvent-accessible from Class II bacteriocins.

The best candidate plantaricin against the SARS-CoV-2 (Table 6) has been identified as the α-subunit of Pln W, as this adhered with ADMET filters, predicted as a potential intranasal drug, interacted with ACE2 and key RBD mutations, mediated covalent interactions with RBD, has the most number of interactions with the lowest binding energy and closest atomic interactions with RBD, especially with Omicron variants. Experimental evidences of the antiviral activity of plantaricin-containing postbiotics such as the strain BS25 CFS and protein fractions, were presented in the next section.

Cytotoxicity Assay

Figure 1 shows the cell viabilities of HEK293T-hACE2 upon treatment with dilutions of the CFS and its crude protein fraction (SGE-CFS), as well as the semi-purified fraction ASP and its crude fraction (SGE-ASP), along with other semi-purified fractions, GAP and HAP8. In the 1:2 dilutions, the viability from CFS is significantly lower than SGE-ASP (p=0.003*). The viabilities from ASP and GAP were significantly lower compared to SGE-CFS (p=0.001** and p=0.012*, respectively). In the 1:4 dilutions, the viability from ASP is significantly lower than CFS and SGE-CFS, (p=0.008** and p=0.004**, respectively). The viability from HAP8 at this dilution is significantly lower compared to SGE-CFS (p=0.0006***). In the 1:8 dilutions, the viability from ASP is significantly lower compared with CFS and SGE-CFS (p=0.001** and p=0.001**, respectively).

Table 3. Molecular Interaction of plantaricins with Key Mutations Found in the RBD

Pln	Bacteriocin class	Pln amino acid and position	Key mutation and position in RBD	SARS-CoV-2 basal strain or variant	Molecular interaction	Atomic distance (Angstrom)
[3]149	I	[1]Tyr 1	[1]Leu 452	Wuhan strain	Hydrophobic contact	1.92
		[2]Ser 2	[1]Leu 452	Wuhan strain	Hydrogen bond	2.35
β-Pln W	I (lanthipeptide)	[1]Ile 3	[1]Asn 405	Omicron BA.4/5	Hydrogen bond	2.55
[3]α-Pln W	I (lanthipeptide)	[2]Asp 14	[2]Lys 440	BA.1	Hydrogen bond	1.78 and 1.72
GZ1-27	II	[1]Val 1	[1,4]Gly 500	Delta variant	Hydrophobic contact	1.92
A	II	[1]Ala 4	[2]Thr 470	BA.1.1.529	Hydrogen bond	2.02
J	II	[2]Arg 21	[1]Leu 452	Wuhan strain	Hydrogen bond	1.91

[1] Hydrophobic residues; [2] Polar or solvent-accessible residues; [3] Predicted as potential intranasal drugs, and [4] Intrinsically disordered region.

Table 4. Covalent Interactions of plantaricins with the RBD

Pln	Bacteriocin class	Pln amino acid and position	Amino acid and position in RBD	SARS-CoV-2 basal strain or variant	Molecular interaction
[3]α-pln W	I (lanthipeptide)	[1]Cys 18	[1]Ile 434	South African	3.14
β-pln W	I (lanthipeptide)	[1]Cys 5	[1,4]Phe 592	D614G	2.42
		[1]Cys 5	[2]Gln 613		2.54
		[2]Arg 30	[1]Cys 430	Delta	3.46
C	I (lanthipeptide)	[1]Cys 26	[1]Cys 430	Delta	3.84
[3]F	II	[1]Gly 34	[1]Cys 432	Omicron BA.1	3.44
3	II	[1]Cys 6	[1]Val 620	Delta	3.32
[3]DL3	II	[1]Ala 8	[1]Cys 590	D614G	3.10
		[2]Thr 10	[1]Cys 590		3.15
Y	II	[2]Ser 1	[1]Cys 432	UK	2.04

[1] Hydrophobic residues; [2] Polar or solvent-accessible residues; [3] Predicted as potential intranasal drugs, and [4] Intrinsically disordered region.

Table 5. Molecular Interaction of plantaricins with ACE2-RBD Binding Sites

Pln	Bacteriocin class	Pln amino acid and position	ACE2 amino acid and position	Molecular interaction	Atomic distance (Angstrom)
[3]a-pln W	I (lanthipeptide)	[2]Asn 6	[2]Asn 51	Hydrogen bond	2.01
		[2]Gln 25	[2]Ser 44	Hydrogen bond	1.96
		[2]Gln 25	[2]Ser 44	Hydrogen bond	2.21
β-pln W	I (lanthipeptide)	[2]Thr 21	[1]Gly 354	Hydrogen bond	1.97
		[2]Lys 29	[1]Trp 349	Hydrogen bond	1.99
C	I (lanthipeptide)	[1]Cys 26	[1]Leu 73	Covalent bond	3.20
[3]F	II	[1]Val 1	[2]Thr 347	Hydrogen bond	2.23
		[2]Ser 6	[2]His 345	Hydrogen bond	1.96
		[2]Ser 6	[2]His 345	Hydrogen bond	2.05
		[1]Ala 7	[2]Thr 347	Hydrogen bond	1.85
3	II	[2]Lys 2	[2,4]Ser 331	Hydrogen bond	2.40
		[2]Ser 3	[2]Asn 330	Hydrogen bond	2.36
		[2]Ser 3	[1,4]Met 332	Hydrogen bond	2.04
		[2]Ser 3	[2]Asn 330	Hydrogen bond	2.01
		[2]Arg 4	[2]Thr 347	Hydrogen bond	2.55
		[2]Arg 5	[2]Thr 347	Hydrogen bond	2.3
		[1]Cys 6	[2]His 345	Covalent bond	3.5
GZ1-27	II	[1]Gly 6	[2]His 345	Hydrogen bond	2.10
		[1]Gly 6	[2]His 345	Hydrogen bond	1.77
J	II	[1]Ala 2	[2]Asp 350	Hydrogen bond	1.92
β-pln S	II	[1]Phe 22	[2]Thr 347	Hydrogen bond	2.21
		[1]Leu 23	[2]Thr 347	Hydrogen bond	2.23

[1] Hydrophobic residues; [2] Polar or solvent-accessible residues; [3] Predicted as potential intranasal drugs, and [4] Intrinsically disordered region.

Table 6. Binding Affinity of the Best Candidate plantaricin to the RBD

Plantaricin (Pln)	Gibbs free energy[1], in ΔG (kCal/mol)	Dissociation constant[2], Kd (M) at 35°C
a-pln W (lanthipeptide) to Omicron BA.4/5 variant RBD	-15.2	1.7×10^{-11}
Control: Tixagevimab (AZD 8895)	-13.8	1.7×10^{-10}
Control: Cilgavimab (AZD 1016)	-12.4	1.5×10^{-9}

Lower values indicate favorable and spontaneous interactions[1], as well as higher affinity and stability[2] of binding, respectively.[4]

Compared with the cell control, the CFS at 1:2 dilution has a significantly lower viability (p=0.0077**). This was also observed in the 1:2, 1:4 and 1:8 dilutions of ASP, 1:2 dilution of GAP, 1:2 and 1:4 dilutions of HAP8, respectively (p<0.0001****, p<0.0001****, p=0.0122*, p=0.0010** and p=0.0083**, respectively). A significant positive correlation occurs for both CFS and GAP (r=0.9971, p=0.03*, thick bars). All dilutions from the crude protein fractions produced 100% cell viability, hence suggesting that the putative peptide does not entail cytotoxicity. Overall, 1:8 dilutions from these samples, except ASP, show either a slight cytotoxicity or no cytotoxicity.

Microneutralization Assay

Activity against nCoV-S-EGFP wild-type Wuhan strain

Figure 2 shows the antiviral activity of the CFS, crude protein and semi-purified fractions in comparison with the positive control, toremifene citrate (TC), against an MOI (0.1) of the nCoV-S-EGFP wt Wuhan strain. The activity of CFS at 1:8 dilution is significantly higher compared with toremifene citrate (TC) (p=0.04*), while HAP8 is significantly lower than CFS (p=0.049*). The activity from ASP at 1:2 dilution is significantly lower with HAP8 at 1:4 dilution (p=0.03*). The activity from both 1:2 and 1:8 dilutions of SGE-ASP were significantly lower compared

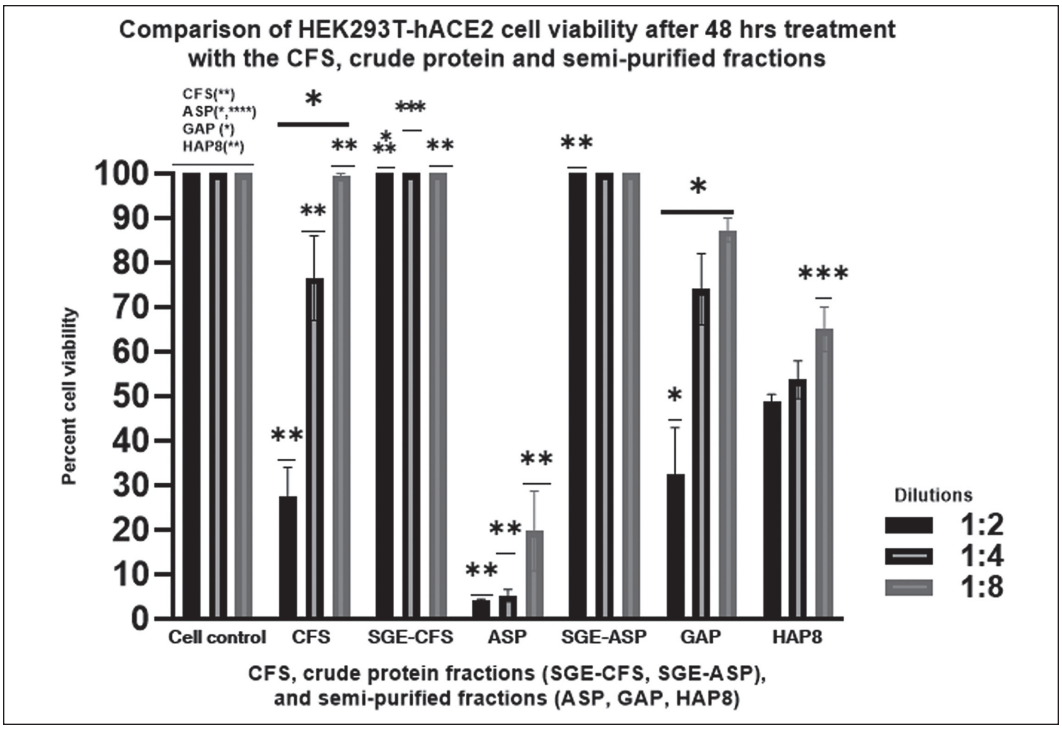

Figure 1. Comparison of the HEK293T-hACE2 percent cell viability with dilutions of the CFS, crude protein and semi-purified fractions. Two-fold dilutions (X-axis) were prepared using the complete media (DMEM-F12-10%FBS). Y-axis pertains to the percent cell viability of after 48 hrs. The MTT assay determines the dilutions from samples which were either cytotoxic (<50% viability) or promote viability (>50%). Each value represents the mean cell viability from a duplicate run in separate microplates. Data were statistically significant at **p* <0.05, ***p* <0.01, ****p* <0.001, and *****p* <0.0001. Error bars indicate mean ± SEM.

Abbreviations: MTT (3-(4,5-Dimethylthiazol-2-yl)-2,5-diphenyl tetrazolium bromide), and DMEM-F12-F10%FBS (Dulbecco's Modified Eagle Medium, with Ham's F12 nutrient mixture and 10% Fetal Bovine Serum). Refer to Methodology for the definition of CFS, SGE-CFS and SGE-ASP, GAP and HAP8.

with CFS (p=0.005** and p=0.01*, respectively). The activity from 1:2 dilution of ASP is significantly higher than SGE-ASP (p=0.02*). The 1:8 dilution of SGE-CFS is significantly lower than CFS (p=0.047*). Overall, the highest neutralizing activity without entailing cytotoxicity can be seen from the 1:8 dilution of CFS.

Activity against nCoV-S-EGFP Omicron BA.1 variant

Figure 3 shows the antiviral activity of the CFS, crude protein and semi-purified fractions in comparison with the positive control, toremifene citrate (TC), against an MOI (0.1) of the nCoV-S-EGFP Omicron BA.1 variant. The activity of CFS at 1:4 and 1:8 dilutions were significantly higher than TC (p=0.02* and p=0.01*, respectively). The activities of ASP and GAP at 1:4 dilutions were significantly higher compared with HAP8 and TC (p=0.008**). The activities from 1:8 dilutions of ASP and GAP respectively, were significantly higher compared with TC (p=0.001** and p=0.006**, respectively). Further, the activities from the 1:8 dilution of ASP and GAP respectively, were significantly higher with HAP8 (p=0.001** and p=0.02*, respectively). The activity from 1:2 dilution of GAP is significantly lower than CFS (p=0.016*) and SGE-ASP (p=0.04*). The activities from 1:4 and 1:8 dilutions of HAP8 were significantly lower compared with CFS, respectively (p=0.037* and p=0.001**, respectively). Also, the activity from 1:4 dilution of HAP8 is significantly lower than SGE-CFS and SGE-ASP (p=0.02*). A significant positive correlation occurs for both CFS and GAP (r=0.998, p=0.03*, thick bar). A significant positive correlation also occurs for both crude protein fractions, SGE-CFS and SGE-ASP (r=0.998, p=0.04*, thick bar). The crude protein fractions also follow the trend with CFS, ASP, GAP and HAP8, *i.e.,* activity becomes higher as dilutions progress, which supports that the antiviral activity is mediated by a peptide. Overall, the highest activities from noncytotoxic dilutions can be seen from 1:4 and 1:8 dilutions of CFS.

Activity against nCoV-S-EGFP wild-type Omicron BA.4/5 variant

Figure 4 shows the antiviral activity of the CFS, semi-purified and crude protein fractions in comparison with the positive control, toremifene citrate (TC), against an MOI (0.1) of the nCoV-S-EGFP Omicron BA.4/5

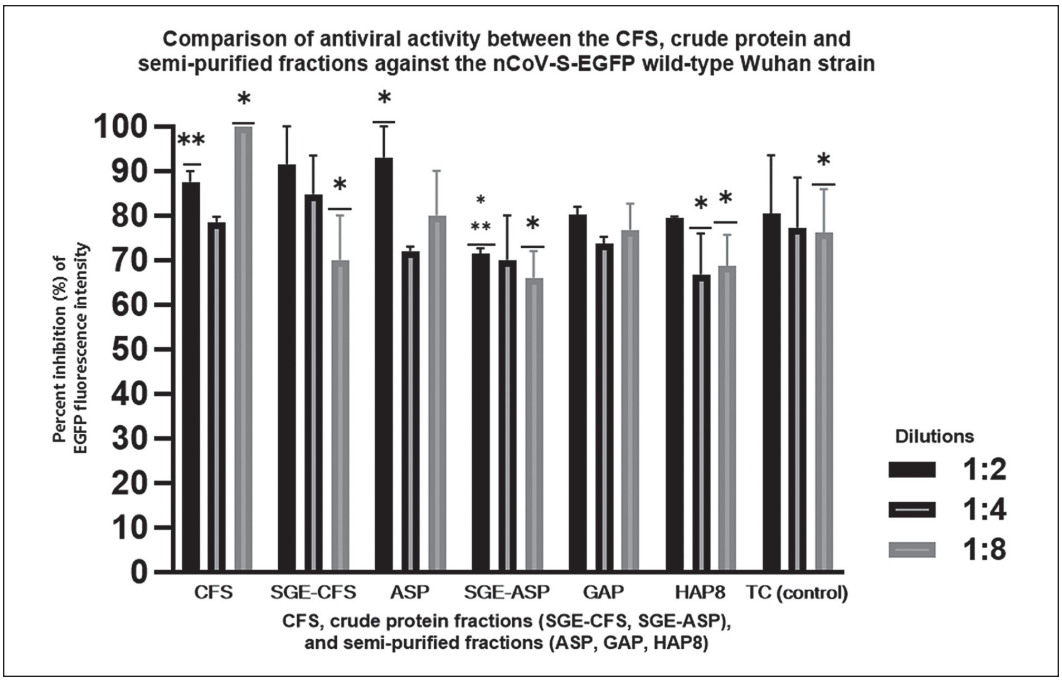

Figure 2. Comparison of the antiviral activity against the nCoV-S-EGFP wild-type Wuhan between the CFS, semi-purified fractions and crude protein fractions. Two-fold dilutions (X-axis) were prepared using the complete media, DMEM-F12-10%FBS. Y-axis indicates the antiviral activity in percent inhibition, expressed as the ratio of the loss of EGFP fluorescence intensity (FI) upon treatment with dilutions of a sample relative to the virus control. The microneutralization assay determines the neutralizing dilutions from samples capable of preventing the viral entry by more than 50% through coincubation with a pseudovirus. Each value represents the mean of a duplicate run performed in separate microplates. Data were statistically significant at **p* <0.05, ***p* <0.01, ****p* <0.001, and *****p* <0.0001. Error bars indicate mean ± SEM.

Abbreviations: nCoV-S-EGFP (Pseudotyped Enhanced Green Fluorescent Protein-labeled Lentivirus expressing the Spike of Novel Coronavirus or a SARS-CoV-2 Spike Pseudotyped Lentivirus) and MOI (multiplicity of infection).

variant. The activities between the crude protein fractions and when compared with the CFS and ASP were parallel, hence further affirms that the antiviral activity is primarily mediated by a peptide. The highest activities can be seen from 1:2, 1:4 and 1:8 dilutions of the CFS, as well as from 1:4 and 1:8 dilutions of ASP. The activities of CFS at 1:4 and 1:8 dilutions were significantly higher than TC (p=0.03* and p=0.02*, respectively). The activity from 1:2 dilution of ASP is significantly higher than GAP (p=0.04*). Also, the activities from 1:4 dilutions of ASP and HAP8, respectively, were significantly higher when compared with TC (p=0.03* and p=0.04*, respectively). The activity from 1:8 dilutions of ASP, GAP and HAP8, respectively, were also significantly higher compared with TC (p=0.01*, p=0.045*, and p=0.04*, respectively). The activities from 1:2 and 1:4 dilutions of GAP were significantly lower than CFS, respectively (p=0.01* and p=0.03*, respectively). The activity from GAP at 1:2 dilution is significantly lower than SGE-CFS and SGE-ASP, respectively (p=0.03* and p=0.009**, respectively). GAP, in the 1:4 dilution, is significantly lower compared with SGE-ASP (p=0.005**).

Across the pseudoviruses, the CFS exhibited 3.24%, 2.17% and 16% higher activities compared with the SGE-CFS at 1:2, 1:4 and 1:8 dilutions, respectively. Overall, the highest neutralizing activities from the CFS, crude protein and semi-purified fractions against the nCoV-S-EGFP wt Wuhan range from 72 to 100% (86.67 ± 4.56, mean ± SEM), while for the nCoV-S-EGFP BA.1 and BA.4/5 variants, range from 78-100% (95.33 ± 3.60) and 90-100% (96.33 ± 2.02), respectively. Generally, the activities of these samples were higher against the BA.4/5 variant followed by the BA.1 variant, then the Wuhan strain. The dilution which exhibited the highest activity taken as an average from all samples is from 1:8 (96.33% ± 2.03), also against the BA.4/5 variant, highlighting their potent activity against this pseudovirus.

Table 7 shows the IC50, CC50 and SI of the CFS, ASP, GAP, HAP8 and TC, against the pseudoviruses. Only the CFS have SI values (>1), highlighting its potential as a therapeutic candidate against live or strains of SARS-CoV-2.[42] This value may reflect a combined action between the metabolites (*e.g.,* organic acids) and the putative peptide. The IC50 and SI values of the samples were also consistent with the trend of activities from the microneutralization assay. Table 8 shows the purification details starting from the CFS. An approximate 55% yield of the putative antiviral peptide was concentrated from the 48-fold purification steps starting

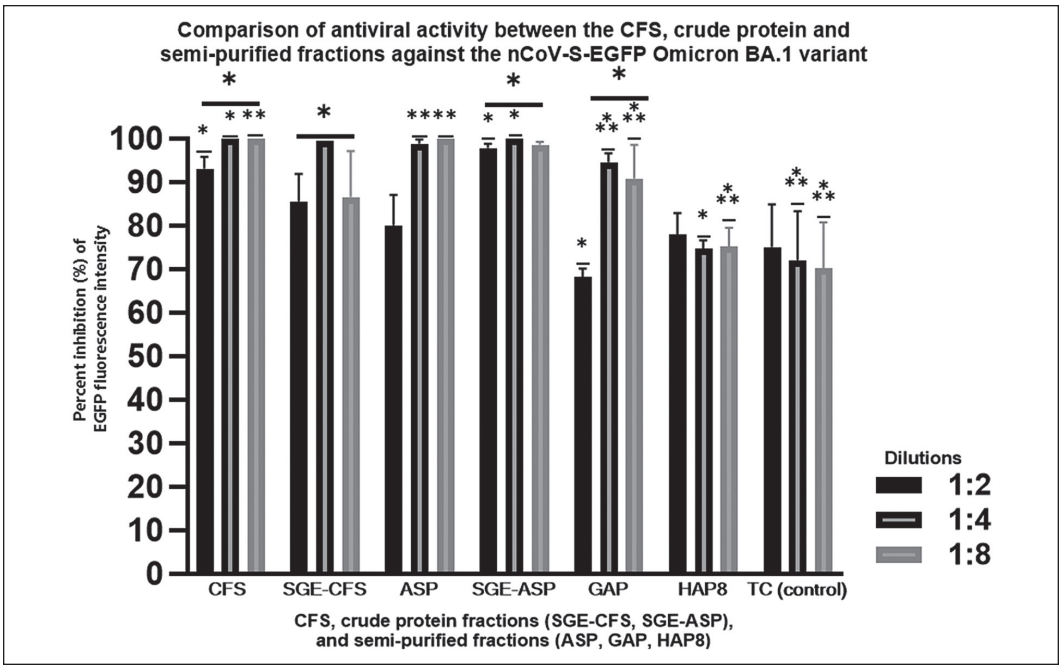

Figure 3. Comparison of the antiviral activity against the nCoV-S-EGFP Omicron BA.1 variant between the CFS, semi-purified fractions and crude protein fractions. Two-fold dilutions (X-axis) were prepared using the complete media, DMEM-F12-10%FBS. Y-axis indicates the antiviral activity in percent inhibition. This assay determines the neutralizing dilutions from samples capable of preventing the viral entry by more than 50% through coincubation with a pseudovirus. Each value represents the mean of a duplicate run performed in separate microplates. Data were statistically significant at $^{*}p$ <0.05, $^{**}p$ <0.01, $^{***}p$ <0.001, and $^{****}p$ <0.0001. Error bars indicate mean ± SEM.

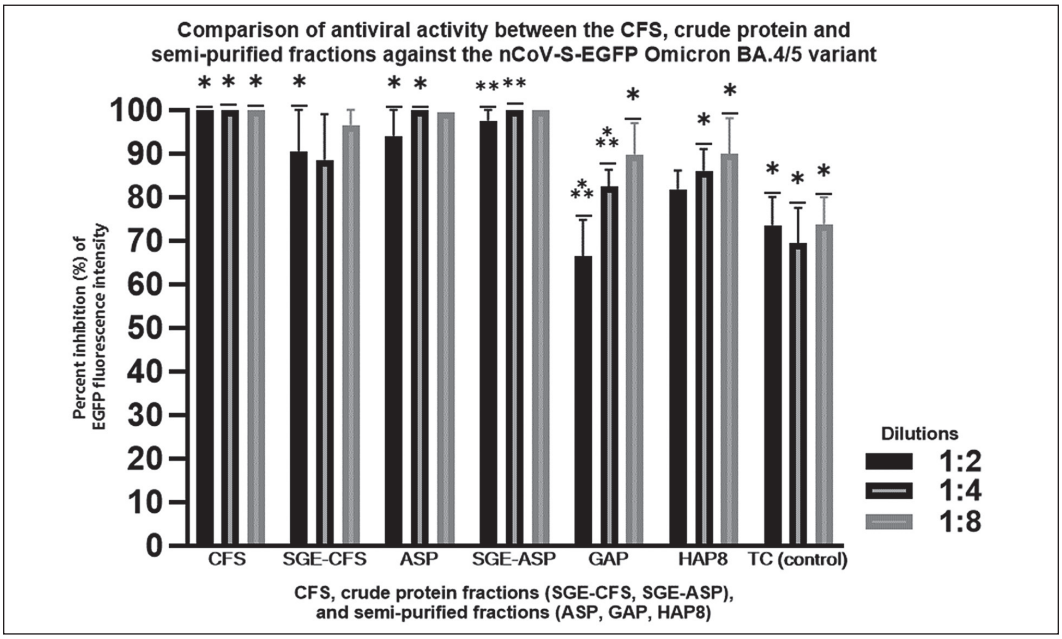

Figure 4. Comparison of the antiviral activity against the nCoV-S-EGFP Omicron BA.4/5 variant between the CFS, crude protein and semi-purified fractions. Two-fold dilutions (X-axis) were prepared using the complete media, DMEM-F12-10%FBS. Y-axis indicates the antiviral activity in percent inhibition. This assay determines the neutralizing dilutions from samples capable of preventing the viral entry by more than 50% through coincubation with a pseudovirus. Each value represents the mean of a duplicate run performed in separate microplates. Data were statistically significant at $^{*}p$ <0.05, $^{**}p$ <0.01, $^{***}p$ <0.001, and $^{****}p$ <0.0001. Error bars indicate mean ± SEM.

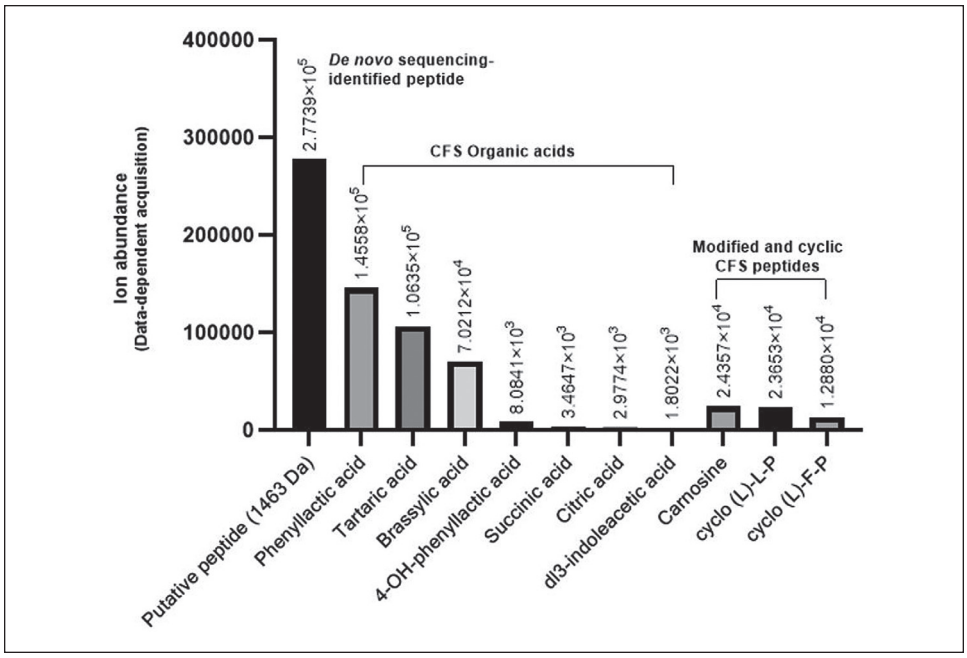

Figure 5. Abundance of the strain BS25 CFS metabolites relevant for antiviral activity, cell viability and cytotoxicity. Actual ion counts vs mass/charge ratio were shown in Y-axis.

Table 7. IC50, CC50 and SI Values of the CFS, ASP, GAP, HAP8, and TC

Samples	CC50	nCoV-S-EGFP wt Wuhan		nCoV-S-EGFP BA.1		nCoV-S-EGFP BA.4/5	
		IC50	SI[1] (CC50/IC50)	IC50	SI[1] (CC50/IC50)	IC50	SI[1] (CC50/IC50)
CFS	2.25	1.26	**1.79**	0.89	**2.53**	0.81	**2.78**
ASP	0.995	3.58	0.28	2.85	0.35	2.36	0.42
GAP	2.63	4.01	0.66	3.16	0.83	4.14	0.64
HAP8	1.22	5.20	0.23	5.37	0.23	3.59	0.34
TC	0.28	8.76	0.03	9.62	0.03	13.64	0.02

[1] *Highlighted were selectivity index values above 1 which indicates a potential therapeutic candidate.*

Table 8. Purification details from the strain BS25 CFS to its semi-purified fractions

Samples	Purification step	Total protein[1] (mg)	Total activity[2] (AU, arbitrary units)	Specific activity[3] (AU/mg)	Purification fold[4]	Percent yield[5]
CFS	Crude cell-free supernatant	0.26	523	641	1	100
ASP	Ammonium sulphate precipitation	0.18	290	1,620	26.93	83
GAP	Pooled gel chromatography	0.294	381	992	45.95	66
HAP8	Semi-preparative RP-HPLC	0.01	375	25,000	47.64	55

[1] *The total protein concentrations identified by Qubit assay were converted to milligrams;*
[2] *Total activity pertains to the reciprocal from the average of dilution factors with highest antiviral activity against nCoV-S-EGFP wt Wuhan, Omicron BA.1 and BA.4/5 variants;*
[3] *Specific activity pertains to the total activity divided by the protein concentration;*
[4] *Purification fold is obtained by dividing specific activity of succeeding fractions from the initial sample, and;*
[5] *Percent yield is calculated by dividing the total activity of the succeeding fraction from the initial sample.*

from the CFS. To identify and screen the main antiviral compound, metabolomics of the CFS has been performed.

Strain BS25 CFS Metabolome

A fraction prepared from the CFS underwent non-targeted metabolomics which has identified organic acids, amino acids and modified forms, sugars, vitamin degradation product, bacterial-derived lipid, enzyme fragment and cyclic peptides (Table 9). The metabolites with potential impacts on cell viability and antiviral activity were quantified through their ion abundances by a data-dependent acquisition (DDA) method (Figure 5), and these include organic acids, modified amino acids and cyclic-peptides, along with a relatively abundant putative peptide.

Suspect Compound Screening

Figure 6 shows bands with an apparent molecular weight of <10 kDa, as seen from the CFS, ASP, individual and pooled gel fractions. The higher loss of antiviral activity upon DTT treatment further supports that the activity is mediated by a peptide with sulfide and thioether bonds, as seen with lanthipeptides (Figure 7).[15,28,42] Table 10 shows the summary of suspect compound screening, which is suggestive only for the presence of plantaricins, possibly mediating the antiviral activity. *De novo* sequencing has identified a putative peptide with the sequence HLCSGDSTCGSTKDM and molecular weight of 1445 Da (1463 Da is the hydrated form). It has been predicted by the RiPPMiner server as a potential lanthipeptide. Database search also revealed no matches, further supporting its putative status. The proposed name of this putative compound is "BS25-JLDM", based on the strain BS25 and investigators, Joshua Mandanas, Leslie Dalmacio, Day Yu Chao, and Marilen Balolong. The *in vitro* evidence of antiviral activity and detection through mass spectrometry, as well as the loss of activity with DTT treatment, possibly imply that the nature of the putative

Table 9. Non-targeted Metabolomics Profile of the Strain BS25 CFS

Metabolite	Observed retention time (seconds)	Observed mass spectra (m/z)	Molecular weight (g/mol)
Putative peptide	217.44	1463 $(1445 + H + H_2O)^+$	1445.00
Organic acids			
Aceturic acid	160.57	117.02	117.10
Succinic acid	158.73	117.20	118.09
Citramalic acid	102.90	146.05	148.11
Tartaric acid	104.27	149.01	150.09
Phenyllactic acid	266.64	165.06	165.17
4-hydroxyphenyllactic acid	443.30	181.05	182.17
Citric acid	165.54	191.02	192.12
dl3-indoleacetic acid	748.84	204.07	203.24
Brassylic acid	971.04	242.18	242.33
Amino acid and modified forms			
Tryptophan	446.38	203.08	204.22
Tyrosine	145.77	180.07	181.19
Phenylalanine	265.40	164.07	165.19
N-acetyl-aspartic acid	139.02	177.04	175.14
O-acetyl-serine	122.71	146.05	147.13
Carnosine	293.83	225.09	226.23
Pyroglutamic acid	146.58	229.12	229.23
Cyclic peptides			
cyclo L-Leucyl-L-Proline	252.83	211.15	210.27
cyclo L-Phenylalanine-D-Proline	272.50	245.13	244.29
cyclo (L)-Valine-leucine-proline-valine-proline	254.87	652.41	651.80
Peptide fragment			
NADH:quinone oxidoreductase	826.38	1122.62	1155.00
Sugars			
Galactose	100.16	179.06	180.16
D-mannitol	781.40	182.99	182.17
Riboflavin degradation product			
7,8-dimethyl alloxazine (lumichrome)	648.79	241.12	242.23
Lipid			
C17-Sphinganine	165.54	288.29	287.50
lysophosphatidylglycerol	667.50	666.35	512.60

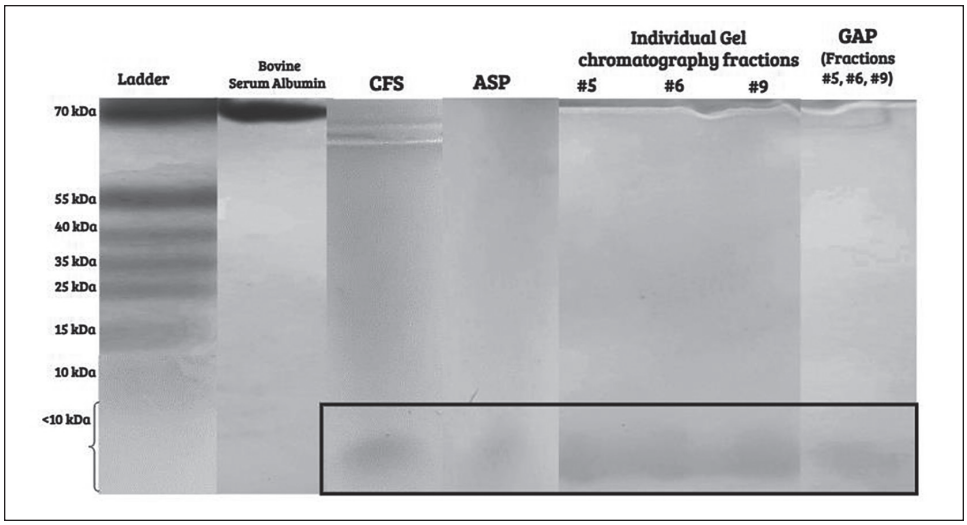

Figure 6. Tris-tricine SDS-PAGE of the CFS, ASP, individual and pooled GAP fractions. Lane 1 pertains to molecular weight markers of the protein ladder (ThermoScientific Page Ruler, 10-70 kDa) with 2 mg of bovine serum albumin (BSA) as the control. Gels were analyzed 72 hrs post-staining with Coomasie blue. Images were color contrasted to greyscale.

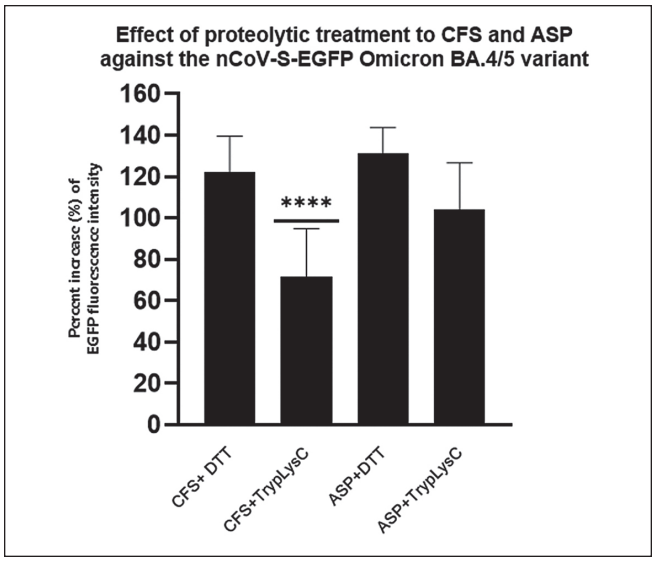

Figure 7. Effect of proteolytic treatment on the antiviral activity of CFS and ASP against the nCoV-S-EGFP Omicron BA.4/5 variant. MOI=0.1 of this pseudovirus was used. Treatment of Dithiothreitol (10 mM) and Trypsin-LysC (100 mM) were performed at 35°C with 5% CO_2 for 3 hrs. The removal of antiviral activity was measured by an increase in EGFP fluorescence intensity (FI) after 48 hrs. The loss of antiviral activity further supports that the antiviral activity of CFS, and possibly the subsequent semi-purified fractions, is mediated by a peptide composed of sulfide or thioether bonds and lysine residues. Each value represents the mean of a duplicate run in separate microplates. Data were statistically significant at $^{*}p$ <0.05, $^{**}p$ <0.01, $^{***}p$ <0.001, and $^{****}p$ <0.0001. Error bars indicate mean ± SEM.

compound is a lanthipeptide, and together, correspond to the level 2 suspect compound screening.[43] Table 11 further supports that the putative peptide has a higher binding affinity for the RBD, especially to the Omicron BA.4/5 variant, compared with ACE2. This affirms the finding from the *in silico* section that a plantaricin lanthipeptide has a higher affinity to the RBD of BA.4/5. In future, level 1 suspect compound confirmation can be achieved through mass spectrometry with a control plantaricin or lanthipeptide along with other biochemical assays and indicator strains.

DISCUSSION

Molecular docking has identified that plantaricins bind more stably with the RBD, compared with ACE2. The larger atomic distance of covalent bonds is due to the radius and electron densities of atoms other than hydrogen.[44] Further, plantaricins can interact with the IDR of RBD and ACE2, these were residues which do not form stable secondary and tertiary structures, allowing interaction with a binding candidate.[45] The best plantaricin candidate, α-Pln W, which is a lanthipeptide, complements Anwar et al., that it interacts with high affinity to the RBD.[17] Together, these support that lanthipeptides from the CFS of *L. plantarum* strains were promising antivirals by preventing SARS-CoV-2 entry.

Non-targeted metabolomics of the strain BS25 CFS has identified a relatively abundant putative peptide along with several compounds with known functional properties, among the organic acids, phenyllactic is the most abundant. It is an antioxidant and known to enhance the activity of lanthipeptides through pH effects.[18] Carnosine, detected in the CFS, is also an antioxidant known to bind residues of ACE2 which were distant from the predicted binding sites of plantaricins.[46] The CFS cyclic peptides, L-Leucyl-L-

Table 10. Suspect compound screen of the putative peptide as the main antiviral metabolite

Sample	Potential presence of plantaricin				*In vitro* activity against the pseudo-viruses	Similar activity with the crude protein fractions	Loss of activity upon proteolytic treatment		*De novo* sequence data
	Detectable protein concentration	Tris-tricine SDS-PAGE (<10 kDa band)	*In vitro* activity against *S. mutans*	Non-lethality to the strain BS25			DTT	Trypsin-LysC	
CFS	Yes	Yes	Yes	Yes	Yes	Yes	Yes	Yes	Yes
ASP	Yes	Yes	Yes	Yes	Yes	Yes	Yes	Yes	Not performed
GAP	Yes	Yes	Yes	Yes	Yes	Yes	Not performed	Not performed	Not performed
HAP8	Yes	Not performed	Not performed	Not performed	Yes	Yes	Not performed	Not performed	Yes

Table 11. Binding affinity of the putative peptide

Target	Binding affinity[1] (kCal/mol)	
	Putative peptide[2] (HLCSGDSTCGSTKDM)	Control: toremifene
RBD of SARS-CoV-2 Wuhan strain	-10.00	-5.60
RBD of SARS-CoV-2 Omicron BA.1 variant	-10.00	-7.08
RBD of SARS-CoV-2 Omicron BA.4/5 variant	-11.40	-5.47
ACE2	-9.97	-6.02

[1] *Lower values indicate favorable and spontaneous interactions*

[2] *Passed ADMET and predicted as a potential intranasal drug*

Proline and L-Phenylalanine-D-Proline, have antifungal and antibacterial properties but were cytotoxic. These can reduce plaque formation by Influenza A.[47] The 1:2 dilution of CFS and all dilutions of ASP were cytotoxic, this may be due to the organic acids succinic, indoleacetic and citric, known to entail cytotoxicities in mammalian cell lines.[48-50] Other CFS organic acids, phenyllactic, tartaric and brassylic, along with carnosine, were known to display antioxidant activities by reduction, chelation and radical scavenging, potentially mediating the cell viability as dilutions progress.[51,52] Traces of ammonium sulfates may also negatively impact the viability from ASP, and together with cytotoxic acids from the CFS, may still be present until the 1:4 dilution of GAP. The CFS is also acidic (pH=4.0), while the ASP and GAP were both slightly acidic (pH=6.0). This is suggestive of the presence of cytotoxic organic acids, whereas the HAP8 and crude fractions, respectively, were within neutral pH (7.0 and 6.8, respectively). The low viabilities seen from HAP8 can be due to trace amounts of RP-HPLC formic acid which is unlikely to mediate any antiviral activity.[53] Overall, 1:8 dilutions of the CFS and GAP have shown no cytotoxicity, which indicates that further dilutions may have neutralized the cytotoxic acids or removed cyclic peptides. To further support this, all dilutions of the crude fractions prepared from both CFS and ASP, namely the SGE-CFS and SGE-ASP, also entail no cytotoxicity, which supports that the putative peptide found in the CFS and fractions can possibly be used as a safe antiviral adjunct on epithelial cells, such as the nasal tract. To note, the putative peptide has no aromatic residues and contains one lysine, hence the decreased absorption of the Coomassie blue dye, which is known to bind with arginine, lysine, and aromatic amino acids.

The aforementioned may have contributed to the appearance of faint bands in the SDS-PAGE.[30,33] In order to ensure the consistency of protein fraction production, an aliquot of the CFS was the source to produce the successive fractions, namely the ASP, GAP and HAP8. The methods were based on optimized antiviral plantaricin purification.[14,17,28,29] Pooling of individual gel chromatography fractions to obtain the GAP, could also impact its higher protein content compared with ASP. Screening tests have indicated a potential plantaricin, especially on the strain BS25 CFS, albeit that the screening was not completely performed on the succeeding fractions, but since the CFS was used to produce these, the finding of potential plantaricin is nevertheless likely to the fractions. Plantaricins were bacteriocin peptides which can be screened initially on samples with detectable protein concentrations, followed by activity on indicator strains and non-lethality to the producing probiotic strain.[15,28] These peptides primarily mediate the antiviral activity observed from *L. plantarum* strains.[13,14]

Infection and neutralization of pseudoviruses compared with live viral strains to ACE2-expressing epithelial cell lines positively correlate and have similar infectivity, hence supports the use of pseudoviruses and HEK293T for COVID-19 drug development, minimizing risks to researchers and environment.[2] The nCoV-S-EGFP Omicron BA.1 variant contains 10 out of 11 wild-type key RBD mutations (no L470T), while the nCoV-S-EGFP BA.4/5 variant contains all the 12 wild-type key RBD mutations, making it more cationic and hydrophobic.[54] Previously, these were the major circulating variants of concern during the experimentation phase of this study (2022-2023). These residues may facilitate interactions with the putative peptide and correlates well

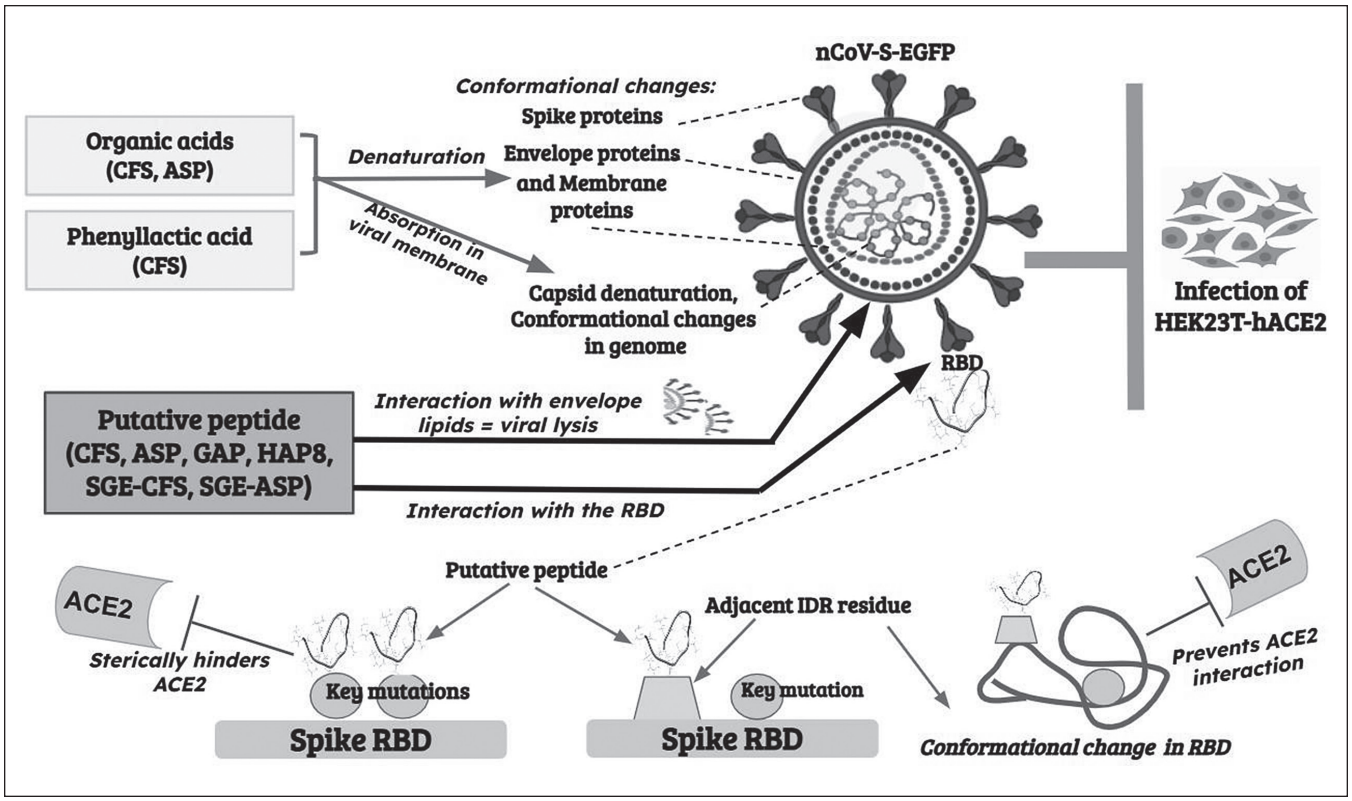

Figure 8. Mechanism of the antiviral activity by the CFS, semi-purified and crude protein fractions.

from the activity of the samples in the microneutralization. The similar trend of activity observed upon coincubation with the pseudoviruses between the CFS, ASP, GAP and HAP8, compared with the crude protein fractions, further support that the activity is mediated by a peptide. The slightly higher activity of the CFS compared with the SGE-CFS implies enhancement of organic acids with the former. Further, the removal of antiviral activity of the CFS and ASP by dithiothreitol, which reversibly reduces thioether or sulfide bonds and dehydrated rings characteristic of lanthipeptides, may have caused conformational changes to the putative peptide, weakening its interaction hence lowered its activity.[29] *De novo* sequencing analysis (PEAKS DB) has indicated the presence of dehydrated serine, threonine and cysteine residues in the putative peptide, which were also apparent to lanthipeptides. These agree with the CFS metabolomics, as the putative peptide predominates, followed by the organic acids. These acids may have enhanced the activity by causing denaturation of the spike, or to the S2, membrane and envelope proteins.[55] The absorption of organic acids by the pseudoviruses leading to capsid denaturation can also be a possibility. Lanthipeptides have been known to interact with negatively charged lipids using their cationic residues followed by permeabilization of their hydrophobic or uncharged residues into the membrane of pathogens.[29] The putative peptide has cationic residues flanking at the amino and carboxy-terminal, while the remainder were "in-between" hydrophobic residues, further suggesting its lytic potential. Analysis on the draft whole genome sequence of the strain BS25 indicates that it can produce plantaricins of class II bacteriocins yet there were no identified lanthipeptide genes.[16] Undetected bacteriocin genes can be encoded by episomal or separate plasmids, as data from WGS may not characterize every plasmids.[56] The possibility of lanthipeptide formation induced by heating of the CFS as performed in this study can also be explored in future. With smaller molecular weights, resistance to extreme temperatures (-20°C to 100°C), ability to be packed into nanocarriers along with the versatility of mechanisms, together support the advantages of lanthipeptide plantaricins as potential antivirals.[57]

The coincubation format utilized in this study allows samples to directly interact with the pseudoviruses, and from this, it can be postulated that the main antiviral metabolite, *i.e.*, the putative peptide, acts as an allosteric competitive inhibitor.[58] This can interact with the active sites (*i.e.*, RBD key mutations) which result in sterically hindering ACE2. The putative peptide can also interact with an IDR residue adjacent to a key RBD mutation (allosteric sites) which caused conformational changes and prevented the interaction with ACE2. Either of these may have prevented a pseudovirus entry hence the absence of EGFP FI (Figure 8). This also correlates with the sustained 100% inhibition and absence of dose dependency. Supplementary docking analysis has indicated that the binding affinity of the

putative peptide is higher with the BA.4/5 variant compared with Wuhan strain, BA.1 variant and ACE2. This further support the substantially higher activity against the BA.4/5 exhibited by the samples. The current circulating SARS-CoV-2 variants from recombinations of Omicron, such as XEC, K.S.1.1 and KP3.3, also have cationic and hydrophobic mutations, suggesting a future application.[59] Together, these point that the activity of the CFS and fractions, is mainly directed against the RBD, and can be utilized as alternative antivirals against SARS-CoV-2 variants. Further exploration on the activity as adjunct antivirals against human and animal pan-coronaviruses, entailing a one-health strategy, can be performed in future investigations.

CONCLUSION

Plantaricins can prevent SARS-CoV-2 entry by interacting with key RBD mutations or with intrinsically disordered RBD residues. The cationic and hydrophobic RBD mutations in the BA.4/5 variant may facilitate interactions with the putative peptide from the CFS and fractions, hence the observed potent activities. These findings can be used as the basis for development of an alternative antiviral targeting the RBD of live or pseudotyped SARS-CoV-2 variants.

Recommendations

Molecular simulations and analysis of the interactions of plantaricins with the SARS-CoV-2 RNA polymerase and protease can be further explored. Desalination of ASP and removal of trace formic acids in HAP8 to improve the viability of HEK293T-hACE2, as well as performing cation-exchange chromatography to increase the yield of the putative peptide, are also recommended. Level 1 confirmation of the suspect compound with a reference plantaricin lanthipeptide can also be explored. Preparation of other crude fractions from GAP and HAP8, tris-tricine SDS-PAGE of HAP8, along with testing the activity of the CFS and semi-purified fractions using a higher multiplicity of infection (MOI) by the pseudoviruses can be performed in future studies. Lastly, the 1:8 dilution of CFS can be utilized against the currently circulating SARS-CoV-2 variants or other pseudotyped strains.

Acknowledgments

The authors acknowledge the University of the Philippines Manila - Applied Microbiology for Health and Environment Research Group (AMHERG) for providing the probiotic strain, as well as the National RNAi Core Facility of Academia Sinica in Taiwan for the pseudoviruses. Further, the authors thank the Graduate Institute of Microbiology and Public Health under the College of Veterinary Medicine of the National Chung Hsing University for hosting the experimentation phase of the study.

Statement of Authorship

All authors certified fulfillment of ICMJE authorship criteria. JAM conceptualized the study, performed experimentations, formal analysis, and wrote the original draft. LMD and DYC provided substantial contributions in the review, editing, analysis, funding, acquisition, and approval of paper. Experimentations were performed in the laboratory of DYC.

Author Disclosure

Funding agencies were not involved in the study design, data analysis, and interpretation, as well as in the decision to submit the article for publication. The authors also declared that there were no relevant financial interests that relate to the research described in this paper.

Funding Source

This study was supported by the Department of Science and Technology – Accelerated Science and Technology Human Resource Development Program (DOST-ASTHRDP).

REFERENCES

1. Wang L, Wang Y, Ye D, Liu Q. Review of the 2019 novel coronavirus (SARS-CoV-2) based on current evidence. Int J Antimicrob Agents. 2020 Jun;55(6):105948. doi: 10.1016/j.ijantimicag.2020.105948. Erratum in: Int J Antimicrob Agents. 2020 Sep;56(3):106137. doi: 10.1016/j.ijantimicag.2020.106137. PMID: 32201353; PMCID: PMC7156162.
2. Zhang F, Li W, Feng J, Ramos da Silva S, Ju E, Zhang H, et al. SARS-CoV-2 pseudovirus infectivity and expression of viral entry-related factors ACE2, TMPRSS2, Kim-1, and NRP-1 in human cells from the respiratory, urinary, digestive, reproductive, and immune systems. J Med Virol. 2021 Dec;93(12):6671-85. doi: 10.1002/jmv.27244. PMID: 34324210; PMCID: PMC8426707.
3. Kalathiya U, Padariya M, Mayordomo M, Lisowska M, Nicholson J, Singh A, et al. Highly conserved homotrimer cavity formed by the SARS-CoV-2 spike glycoprotein: a novel binding site. J Clin Med. 2020 May 14;9(5):1473. doi: 10.3390/jcm9051473. PMID: 32422996; PMCID: PMC7290299.
4. Lau SY, Wang P, Mok BW, Zhang AJ, Chu H, Lee AC, et al. Attenuated SARS-CoV-2 variants with deletions at the S1/S2 junction. Emerg Microbes Infect. 2020 Dec;9(1):837-42. doi: 10.1080/22221751.2020.1756700. PMID: 32301390; PMCID: PMC7241555.
5. Tegally H, Moir M, Everatt J, Giovanetti M, Scheepers C, Wilkinson E, et al. Emergence of SARS-CoV-2 Omicron lineages BA.4 and BA.5 in South Africa. Nat Med. 2022 Sep;28(9):1785-90. doi: 10.1038/s41591-022-01911-2. PMID: 35760080; PMCID: PMC9499863.
6. Jeon S, Ko M, Lee J, Choi I, Byun SY, Park S, et al. Identification of antiviral drug candidates against SARS-CoV-2 from FDA-approved drugs. Antimicrob Agents Chemother. 2020 Jun 23;64(7):e00819-20. doi: 10.1128/AAC.00819-20. PMID: 32366720; PMCID: PMC7318052.
7. Ader F, Bouscambert-Duchamp M, Hites M, Peiffer-Smadja N, Poissy J, Belhadi D, et al. Remdesivir plus standard of care versus standard of care alone for the treatment of patients admitted to hospital with COVID-19 (DisCoVeRy): a phase 3, randomised, controlled, open-label trial. Lancet Infect Dis. 2022 Feb;22(2):209-21. doi: 10.1016/S1473-3099(21)00485-0. PMID: 34534511; PMCID: PMC8439621.

8. Butler CC, Hobbs FDR, Gbinigie OA, Rahman NM, Hayward G, Richards DB, et al. PANORAMIC Trial Collaborative Group. Molnupiravir plus usual care versus usual care alone as early treatment for adults with COVID-19 at increased risk of adverse outcomes (PANORAMIC): an open-label, platform-adaptive randomised controlled trial. Lancet. 2023 Jan 28;401(10373):281-293. doi: 10.1016/S0140-6736(22)02597-1. PMID: 36566761; PMCID: PMC9779781.
9. Edelstein GE, Boucau J, Uddin R, Marino C, Liew MY, Barry M, et al. SARS-CoV-2 virologic rebound with nirmatrelvir-ritonavir therapy: an observational study. Ann Intern Med. 2023 Dec;176(12):1577-85. doi: 10.7326/M23-1756. Erratum in: Ann Intern Med. 2024 Apr;177(4):547. doi: 10.7326/L24-0045. PMID: 37956428; PMCID: PMC10644265.
10. Mehra R. Selective Estrogen Modulation and Melatonin in Early COVID-19 (SENTINEL). ClinicalTrials.gov identifier: NCT04531748. ClinicalTrials.gov [Internet]. 2021-05-10 [cited 2026 Feb]. Available from: https://clinicaltrials.gov/study/NCT04531748
11. Nguyen H, Lan PD, Nissley DA, O'Brien EP, Li MS. Cocktail of REGN antibodies binds more strongly to SARS-CoV-2 than its components, but the Omicron Variant reduces its neutralizing ability. J Phys Chem B. 2022 Apr 21;126(15):2812-2823. doi: 10.1021/acs.jpcb.2c00708. PMID: 35403431; PMCID: PMC9016775.
12. Rocchetti MT, Russo P, Capozzi V, Drider D, Spano G, Fiocco D. Bioprospecting antimicrobials from Lactiplantibacillus plantarum: Key factors underlying its probiotic action. Int J Mol Sci. 2021 Nov 8;22(21):12076. doi: 10.3390/ijms222112076. PMID: 34769500; PMCID: PMC8585029.
13. Kim SW, Kang SI, Shin DH, Oh SY, Lee CW, Yang Y, et al. Potential of cell-free supernatant from Lactobacillus plantarum NIBR97, including novel bacteriocins, as a natural alternative to chemical disinfectants. Pharmaceuticals (Basel). 2020 Sep 23;13(10):266. doi: 10.3390/ph13100266. PMID: 32977547; PMCID: PMC7650660.
14. Rather IA, Choi SB, Kamli MR, Hakeem KR, Sabir JSM, Park YH, et al. Potential adjuvant therapeutic effect of Lactobacillus plantarum Probio-88 postbiotics against SARS-COV-2. Vaccines (Basel). 2021 Sep 24;9(10):1067. doi: 10.3390/vaccines9101067. PMID: 34696175; PMCID: PMC8537773.
15. Banaay CGB, Elegado FB, Dalmacio IF. Identification and characterization of bacteriocinogenic Lactobacillus plantarum BS25 isolated from Balao-balao, a locally fermented rice-shrimp mixture from the Philippines. Phil Agri Sci. 2021;87:427–38.
16. Lara ZB, Amoranto MBC, Elegado FB, Dalmacio LMM, Balolong MP. Draft genome sequence of Lactiplantibacillus plantarum BS25 isolated from a local fermented rice-shrimp mixture from the Philippines. Microbiol Resour Announc. 2024 Feb 15;13(2):e0080823. doi: 10.1128/mra.00808-23. PMID: 38179907; PMCID: PMC10868257.
17. Anwar F, Altayb HN, Al-Abbasi FA, Al-Malki AL, Kamal MA, Kumar V. Antiviral effects of probiotic metabolites on COVID-19. J Biomol Struct Dyn. 2021 Jul;39(11):4175-84. doi: 10.1080/07391102.2020.1775123. PMID: 32475223; PMCID: PMC7298884.
18. Liu J, Huang R, Song Q, Xiong H, Ma J, Xia R, et al. Combinational antibacterial activity of nisin and 3-phenyllactic acid and their co-production by engineered Lactococcus lactis. Front Bioeng Biotechnol. 2021 Feb 5;9:612105. doi: 10.3389/fbioe.2021.612105. PMID: 33634085; PMCID: PMC7901885.
19. Sunmola AA, Ogbole OO, Faleye TOC, Adetoye A, Adeniji JA, Ayeni FA. Antiviral potentials of Lactobacillus plantarum, Lactobacillus amylovorus, and Enterococcus hirae against selected Enterovirus. Folia Microbiol (Praha). 2019 Mar;64(2):257-64. doi: 10.1007/s12223-018-0648-6. PMID: 30267215.
20. Arena MP, Elmastour F, Sane F, Drider D, Fiocco D, Spano G, et al. Inhibition of coxsackievirus B4 by Lactobacillus plantarum. Microbiol Res. 2018 May;210:59-64. doi: 10.1016/j.micres.2018.03.008. PMID: 29625659.
21. Yang Y, Song H, Wang L, Dong W, Yang Z, Yuan P, et al. Antiviral effects of a probiotic metabolic products against transmissible gastroenteritis coronavirus. J Prob Health. 5: 184. doi: 10.4172/2329-8901.1000184.
22. Rather IA, Choi KH, Bajpai VK, Park YH. Antiviral mode of action of Lactobacillus plantarum YML009 on influenza virus H1N1. Bangladesh J Pharmacol. 2015;10:475-82. doi: 10.3329/bjp.v10i2.23068.
23. Ritchie TJ, Luscombe CN, Macdonald SJ. Analysis of the calculated physicochemical properties of respiratory drugs: can we design for inhaled drugs yet? J Chem Inf Model. 2009 Apr;49(4):1025-32. doi: 10.1021/ci800429e. PMID: 19275169.
24. Kozakov D, Hall DR, Xia B, Porter KA, Padhorny D, Yueh C, et al. The ClusPro web server for protein-protein docking. Nat Protoc. 2017 Feb;12(2):255-78. doi: 10.1038/nprot.2016.169. PMID: 28079879; PMCID: PMC5540229.
25. Sobiesk JL, Munakomi S. Anatomy, Head and Neck, Nasal Cavity. 2023 Jul 24. In: StatPearls [Internet]. Treasure Island (FL): StatPearls Publishing; 2025 Jan. PMID: 31334952.
26. Mandanas JAH, Dalmacio LMM, Balolong MP. Activity of putative bacteriocins from Lactobacillus plantarum B25 and Pediococcus acidilactici S3 against antibiotic-resistant Vibrio spp. Poster Proceeding from the 47th Annual Convention of the Philippine Society of Biochemistry and Molecular Biology: Virtual International Conference; Dec 1-4, 2020; PSBMB Central Luzon Chapter, Philippines. Poster identifier: H-06.
27. Reynolds J. Serial Dilution Protocols. American Society of Microbiology. ASM [Internet]. 30-09-2005 [cited 2026 Feb]. Available from: https://asm.org/asm/media/protocol-images/serial-dilution-protocols.pdf?ext=.pdf
28. Wang Y, Qin Y, Xie Q, Zhang Y, Hu J, Li P. Purification and characterization of plantaricin LPL-1, a novel class IIa bacteriocin produced by Lactobacillus plantarum LPL-1 isolated from fermented fish. Front Microbiol. 2018 Sep 28;9:2276. doi: 10.3389/fmicb.2018.02276. PMID: 30323792; PMCID: PMC6172451.
29. Holo H, Jeknic Z, Daeschel M, Stevanovic S, Nes IF. Plantaricin W from Lactobacillus plantarum belongs to a new family of two-peptide lantibiotics. Microbiology (Reading). 2001 Mar;147(Pt 3):643-51. doi: 10.1099/00221287-147-3-643. PMID: 11238971.
30. Šeatović SL, Novaković JS, Zavišić GN, Radulović ŽC, Gavrović-Jankulović MD, Jankov RM. The partial characterization of the antibacterial peptide bacteriocin G2 produced by the probiotic bacteria Lactobacillus plantarum G2. J Serb Chem Soc. 2011;76:699–707. doi: 10.2298/JSC100605060S
31. Maldonado A, Jiménez-Díaz R, Ruiz-Barba JL. Induction of plantaricin production in Lactobacillus plantarum NC8 after coculture with specific gram-positive bacteria is mediated by an autoinduction mechanism. J Bacteriol. 2004 Mar;186(5):1556-64. doi: 10.1128/JB.186.5.1556-1564.2004. PMID: 14973042; PMCID: PMC344433.
32. Lin X, Xu J, Shi Z, Xu Y, Fu T, Zhang L, et al. Evaluation of the antibacterial effects and mechanism of Plantaricin 149 from Lactobacillus plantarum NRIC 149 on the peri-implantitis pathogens. Sci Rep. 2021 Oct 25;11(1):21022. doi: 10.1038/s41598-021-00497-y. PMID: 34697350; PMCID: PMC8545926.
33. Schägger H. Tricine-SDS-PAGE. Nat Protoc. 2006;1(1):16-22. doi: 10.1038/nprot.2006.4. PMID: 17406207.
34. Wang W, He J, Pan D, Wu Z, Guo Y, Zeng X, et al. Metabolomics analysis of Lactobacillus plantarum ATCC 14917 adhesion activity under initial acid and alkali stress. PLoS One. 2018 May 24;13(5):e0196231. doi: 10.1371/journal.pone.0196231. PMID: 29795550; PMCID: PMC5967736.
35. Pérez-Ramos A, Madi-Moussa D, Coucheney F, Drider D. Current knowledge of the mode of action and immunity mechanisms of LAB-bacteriocins. Microorganisms. 2021 Oct 7;9(10):2107. doi: 10.3390/microorganisms9102107. PMID: 34683428; PMCID: PMC8538875.

36. Flórez AB, Mayo B. Genome analysis of Lactobacillus plantarum LL441 and genetic characterisation of the locus for the Lantibiotic Plantaricin C. Front Microbiol. 2018 Aug 17;9:1916. doi: 10.3389/fmicb.2018.01916. PMID: 30174666; PMCID: PMC6107846.
37. Vista FES, Dalmacio LMM, Corales LGM, Salem GM, Galula JU, Chao DY. Antiviral effect of crude aqueous extracts from ten Philippine medicinal plants against zika virus. Acta Med Philipp. 2020;54(2):195-202. doi: 10.47895/amp.v54i2.1501.
38. Lin WS, Chen IC, Chen HC, Lee YC, Wu SC. Glycan masking of epitopes in the NTD and RBD of the spike protein elicits broadly neutralizing antibodies against SARS-CoV-2 variants. Front Immunol. 2021 Dec 2;12:795741. doi: 10.3389/fimmu.2021.795741. PMID: 34925381; PMCID: PMC8674692.
39. Zhou W, Xu C, Wang P, Anashkina AA, Jiang Q. Impact of mutations in SARS-COV-2 spike on viral infectivity and antigenicity. Brief Bioinform. 2022 Jan 17;23(1):bbab375. doi: 10.1093/bib/bbab375. PMID: 34518867; PMCID: PMC8499914.
40. Zumdahl S. Chemical Principles. 5th Edition. Houghton Miffin; 2004.
41. Du X, Li Y, Xia YL, Ai SM, Liang J, Sang P, et al. Insights into protein-ligand interactions: mechanisms, models, and methods. Int J Mol Sci. 2016 Jan 26;17(2):144. doi: 10.3390/ijms17020144. PMID: 26821017; PMCID: PMC4783878.
42. Xiao X, Wang C, Chang D, Wang Y, Dong X, Jiao T, et al. Identification of potent and safe antiviral therapeutic candidates against SARS-CoV-2. Front Immunol. 2020 Nov 25;11:586572. doi: 10.3389/fimmu.2020.586572. PMID: 33324406; PMCID: PMC7723961.
43. Schymanski EL, Jeon J, Gulde R, Fenner K, Ruff M, Singer HP, et al. Identifying small molecules via high resolution mass spectrometry: communicating confidence. Environ Sci Technol. 2014 Feb 18;48(4):2097-8. doi: 10.1021/es5002105. PMID: 24476540.
44. Nordholm S, Bacskay G. The basics of covalent bonding in terms of energy and dynamics. Molecules. 2020 Jun 8;25(11):2667. doi: 10.3390/molecules25112667. PMID: 32521828; PMCID: PMC7321125.
45. Babu MM. The contribution of intrinsically disordered regions to protein function, cellular complexity, and human disease. Biochem Soc Trans. 2016 Oct 15;44(5):1185-200. doi: 10.1042/BST20160172. PMID: 27911701; PMCID: PMC5095923.
46. Saadah LM, Deiab GIA, Al-Balas Q, Basheti IA. Carnosine to combat novel coronavirus (nCoV): molecular docking and modeling to cocrystallized host angiotensin-converting enzyme 2 (ACE2) and viral spike protein. Molecules. 2020 Nov 28;25(23):5605. doi: 10.3390/molecules25235605. PMID: 33260592; PMCID: PMC7730390.
47. Kwak MK, Liu R, Kwon JO, Kim MK, Kim AH, Kang SO. Cyclic dipeptides from lactic acid bacteria inhibit proliferation of the influenza A virus. J Microbiol. 2013 Dec;51(6):836-43. doi: 10.1007/s12275-013-3521-y. PMID: 24385362.
48. Giardino L, Generali L, Savadori P, Barros MC, de Melo Simas LL, Pytko-Polończyk J, et al. Can the concentration of citric acid affect its cytotoxicity and antimicrobial activity? Dent J (Basel). 2022 Aug 9;10(8):148. doi: 10.3390/dj10080148. PMID: 36005246; PMCID: PMC9406502.
49. Kasarci G, Ertugrul B, Iplik ES, Cakmakoglu B. The apoptotic efficacy of succinic acid on renal cancer cell lines. Med Oncol. 2021 Oct 23;38(12):144. doi: 10.1007/s12032-021-01577-9. PMID: 34687367.
50. Kurokawa H, Taninaka A, Shigekawa H, Matsui H. Dabigatran etexilate induces cytotoxicity in rat gastric epithelial cell line via mitochondrial reactive oxygen species production. Cells. 2021 Sep 22;10(10):2508. doi: 10.3390/cells10102508. PMID: 34685491; PMCID: PMC8533938.
51. Suriyaprom S, Mosoni P, Leroy S, Kaewkod T, Desvaux M, Tragoolpua Y. Antioxidants of fruit extracts as antimicrobial agents against pathogenic bacteria. Antioxidants (Basel). 2022 Mar 21;11(3):602. doi: 10.3390/antiox11030602. PMID: 35326252; PMCID: PMC8945554.
52. Tyagi A, Shabbir U, Chelliah R, Daliri EB, Chen X, Oh DH. Limosilactobacillus reuteri fermented brown rice: a product with enhanced bioactive compounds and antioxidant potential. Antioxidants (Basel). 2021 Jul 5;10(7):1077. doi: 10.3390/antiox10071077. PMID: 34356310; PMCID: PMC8301027.
53. Treichel JL, Henry MM, Skumatz CM, Eells JT, Burke JM. Antioxidants and ocular cell type differences in cytoprotection from formic acid toxicity in vitro. Toxicol Sci. 2004 Nov;82(1):183-92. doi: 10.1093/toxsci/kfh256. PMID: 15319487.
54. Academia Sinica: Information on the nCoV-S-EGFP Pseudoviruses. RNAi Core Facility [Internet]. Jan 2024 [cited 2026 Feb]. Available from: https://rnai.genmed.sinica.edu.tw/index.html.
55. Zhao X, Chen H, Wang H. Glycans of SARS-CoV-2 Spike protein in virus infection and antibody production. Front Mol Biosci. 2021 Apr 13;8:629873. doi: 10.3389/fmolb.2021.629873. PMID: 33928117; PMCID: PMC8076860.
56. Golneshin A, Gor MC, Williamson N, Vezina B, Van TTH, May BK, et al. Discovery and characterisation of circular bacteriocin plantacyclin B21AG from Lactiplantibacillus plantarum B21. Heliyon. 2020 Aug 21;6(8):e04715. doi: 10.1016/j.heliyon.2020.e04715. PMID: 32904251; PMCID: PMC7452424.
57. Fu Y, Jaarsma AH, Kuipers OP. Antiviral activities and applications of ribosomally synthesized and post-translationally modified peptides (RiPPs). Cell Mol Life Sci. 2021 Apr;78(8):3921-40. doi: 10.1007/s00018-021-03759-0. PMID: 33532865; PMCID: PMC7853169.
58. Strelow J, Dewe W, Iversen PW, Brooks HB, Radding JA, McGee J, et al. Mechanism of Action Assays for Enzymes. 2012 May 1 [updated 2012 Oct 1]. In: Markossian S, Grossman A, Baskir H, Arkin M, Auld D, Austin C, et al. Assay Guidance Manual [Internet]. Bethesda (MD): Eli Lilly & Company and the National Center for Advancing Translational Sciences; 2004. PMID: 22553872.
59. Waafira A, Subbaram K, Faiz R, Naher ZU, Manandhar PL, Ali S. A new and more contagious XEC subvariant of SARS-CoV-2 may lead to massive increase in COVID-19 cases. New Microbes New Infect. 2024 Oct 24;62:101517. doi: 10.1016/j.nmni.2024.101517. PMID: 39525491; PMCID: PMC11546678.